

Comparison of the structure of the plasma-facing surface and tritium accumulation in beryllium tiles from JET ILW campaigns 2011–2012 and 2013–2014



Elina Pajuste^{a,*}, Gunta Kizane^a, Ieva Igaune^a, Liga Avotina^a, Jet Contributors^{b,1}

^a Institute of Chemical Physics, University of Latvia, Jelgavas St.1, Riga, LV 1004, Latvia

^b EUROfusion Consortium, JET, Culham Science Centre, Abingdon, OX14 3DB, UK

ARTICLE INFO

Keywords:

Tritium
Beryllium
ITER-like wall
Joint European Torus
Fuel retention

ABSTRACT

In this study, beryllium tiles from Joint European Torus (JET) vacuum vessel wall were analysed and compared regarding their position in the vacuum vessel and differences in the exploitation conditions during two campaigns of ITER-Like-Wall (ILW) in 2011–2012 (ILW1) and 2013–2014 (ILW2)

Tritium content in beryllium samples were assessed. Two methods were used to measure tritium content in the samples – dissolution under controlled conditions and tritium thermal desorption. Prior to desorption and dissolution experiments, scanning electron microscopy and energy dispersive x-ray spectroscopy were used to study structure and chemical composition of plasma-facing-surfaces of the beryllium samples.

Experimental results revealed that tritium content in the samples is in range of $2 \cdot 10^{11}$ – $2 \cdot 10^{13}$ tritium atoms per square centimetre of the surface area with its highest content in the samples from the outer wall of the vacuum vessel (up to $1.9 \cdot 10^{13}$ atoms/cm² in ILW1 campaign and $2.4 \cdot 10^{13}$ atoms/cm² in ILW2). The lowest content of tritium was found in the upper part of the vacuum vessel ($2.0 \cdot 10^{12}$ atoms/cm² and $2.0 \cdot 10^{11}$ atoms/cm² in ILW1 and ILW2, respectively).

Results obtained from scanning electron microscopy has shown that surface morphology is different within single tile, however if to compare two campaigns main tendencies remains similar.

1. Introduction

ITER-Like Wall (ILW) project has been carried out at Joint European Torus JET to test plasma facing materials relevant to International Thermonuclear Experimental Reactor – ITER. During regular shut-downs material samples are retrieved for off-situ analysis.

The first wall of the JET vacuum vessel is made of bulk beryllium tiles, whereas for the divertor bulk tungsten and tungsten coated carbon fibre composite tiles are used [1].

Beryllium choice is based on its low Z, good thermal conductivity, and high oxygen gettering characteristics. Beryllium has been tested as a plasma facing material also in earlier experiments in JET with its first introduction in 1989 and also in smaller early period tokamaks such as UNITOR and ISX-B [2]. However, this is the first time when combination of materials planned in ITER are tested together.

Main issues related to the performance of plasma facing materials are erosion and fuel accumulation. Thermal transient loads cause

heating of beryllium surface and results in significant changes – material loss, melting, cracking, evaporation, formation of dust. To assess the erosion of beryllium components so-called marker tiles are being used in JET where regular beryllium tile is coated first with nickel film (2–3 μm) acting as an interlayer and then with a Be layer (7–10 μm) [3–5].

Fuel retention in the plasma facing materials is both economical and radiological issue due to tritium (T) radioactivity. Tritium in-vessel inventory limitation of 700 g have been set for ITER [6].

During the first two ILW campaigns, ILW1 and ILW2, only stable hydrogen isotopes (protium H and deuterium D) have been introduced in the vacuum vessel of JET, however there are several possible sources of tritium in the beryllium wall materials: in-vessel tritium inventory remaining from previous D – T campaigns, energetic tritium ion production as a results of D – D reaction and tritium production in neutron induced transmutation of beryllium.

There have been three campaigns in JET when tritium was

* Corresponding author.

E-mail address: elina.pajuste@lu.lv (E. Pajuste).

¹ See author list in the paper, X. Litaudon et al., Nucl. Fusion, 57 (2017) 102001

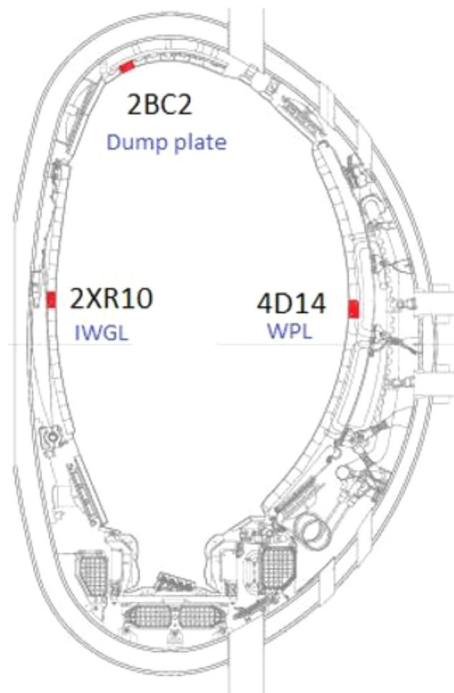
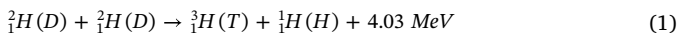


Fig. 1. Cross section of JET vacuum vessel indicating the position of the analysed tiles.

introduced in the vacuum vessel: Preliminary Tritium Experiment (PTE) in 1991 [7] the first Deuterium-Tritium Experiment (DTE1) in 1997 [8,9] and the Trace Tritium Experiment (TTE) in 2003 [10]. In total 420 mg of tritium has been introduced (5 mg – PTE, 35 mg – DTE1 and 380 mg – TTE) [11]. Tritium gas present in the vessel can accumulate in the first wall materials as a result of co-deposition with eroded materials and by physical diffusion into the bulk of wall material. Co-deposited tritium could be expected to be retained in near surface of the plasma facing material, however tritium as a hydrogen isotope is very mobile due to its small size and might diffuse much deeper into the bulk. Such parameters as solubility, trapping energies and diffusivity plays significant role in estimation of tritium diffusion depth. Theoretical model of hydrogen trapping on the imperfections of the lattice, such as vacancies, grain boundaries, etc. has been described [12]. Some properties might be extrapolated from available data about protium or deuterium, however, isotopic effects must be taken into account [13]. Comprehensive overview of the experimentally obtained data on hydrogen solubility, diffusivity and permeation has been provided by R. A. Causey in 2002 [14].

Tritium can be produced in vacuum vessel also as a product of the D–D fusion reaction (1).



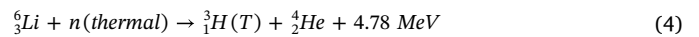
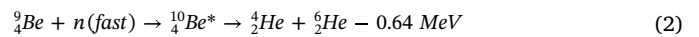
Third source of tritium in beryllium that will play significant role in

Table 1

List of analysed samples and their position in the tiles (LH-left hand, RH-right hand).

Tile	Position in tile	Sample number	
		ILW1	ILW2
IWGL – 2XR10	LH center	60	263
	Center	41	207
	RH center	28	195
	RH wing	74	178
WPL – 4D14	LH wing	165	365
	LH intermid.	151	351
	Centre	130	330
	RH intermid.	114	314
	RH wing	106	306
DP-2BC2	RH	79	279

the future fusion devices is neutron induced transmutation of beryllium. An example of Be transmutation chain where tritium can be produced is given in the following reactions 2–4 [15].



Tritium production and behaviour in neutron irradiated beryllium have been studied widely regarding beryllium application in tritium breeding units where it is foreseen as neutron multiplier [16]. However, it must be emphasized that overall neutron yield in ILW1 and ILW2 are very low ($\sim 5 \cdot 10^{19}$ neutrons in total) and the dominant source of tritium can be considered previous D – T experiments.

In this study, beryllium materials from the first two campaigns ILW1 (2012–2013) and ILW2 (2013–2014) are analysed and compared regarding their plasma facing surface microstructure and accumulated tritium.

2. Material and methods

2.1. Samples

During the shutdowns in 2012 (ILW1) and 2014 (ILW2), selected beryllium tiles were removed from the following positions of the vacuum vessel - inner wall (Inner Wall Guarding Limiter - IWGL), outer wall (Wide Poloidal Limiter - WPL) and upper vessel part (Dump Plate - DP). Samples of approximately $1.2 \times 1.2 \times 1.0 \text{ cm}^3$ cut out of tiles (as described in [17]) were used in the present study. These samples were further cut into two parts in order to perform tritium depth profiling and desorption experiments. Samples from identical positions in the vacuum vessel and each particular tile were analysed from both shutdowns to ensure reliable comparison of the two campaigns. Position of the analysed tiles in the vacuum vessel are shown in the Fig. 1 and position of the samples cut out of the tiles in Fig. 2, whereas detailed list of the samples in Table 1.

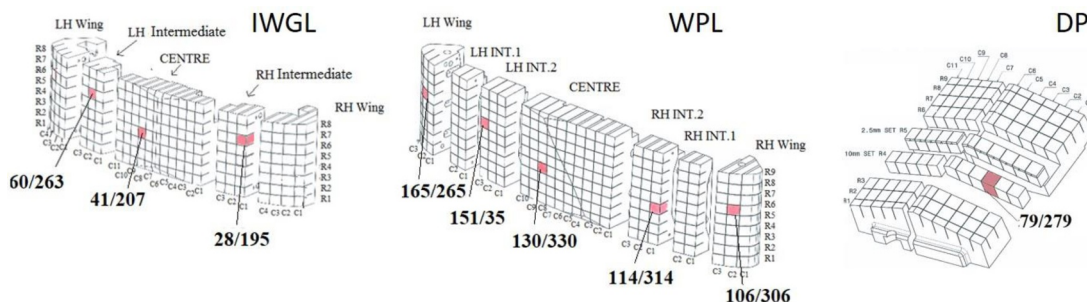


Fig. 2. Position of the samples cut out of the tiles.

Table 2
Comparison of ITER – Like – Wall first two campaigns - ILW1 and ILW 2 [5].

Campaign	Number of discharges	Total discharge time, 10 ⁴ s	Total input energy, GJ	H injection	D injection
ILW1	3812	6.41	150.6	2.726·10 ²⁴	2.518·10 ²⁶
ILW2	4150	7.12	200.5	3.035·10 ²⁵	3.721·10 ²⁶

During the ILW2 campaign injected power to the plasma discharges was higher and strike point position different if to compare with ILW1, that might cause differences both regarding the wall material behaviour and the amount of accumulated fuel. For example, there were observed lower beryllium erosion in ILW2 than that in ILW1 [5]. Another significant difference regarding fuel is that ILW2 was ended with H-fuelled campaign (10% of the total number of pulse) whereas ILW1 was predominately a D-fuelled plasma campaign [18]. Comparison of the two campaigns are given in the Table 2.

2.2. Tritium measurements

Tritium total content in the samples was measured by two methods - beryllium dissolution and thermal desorption spectroscopy.

Dissolution method developed for tritium measurement in bulk beryllium gives possibility to assess also tritium depth profile that has been published previously [19,20]. In this method, successive layers of

Be were removed using 1 mol/L sulphuric acid and amount of evolved hydrogen and released tritium trapped in the material measured. Molecular and atomic (interstitial) tritium present in a Be sample transfers into a flow of carrier gas (Ar, 8.0–8.5 L/h), where tritium activity was measured by proportional counter with an operating volume of 300 cm³ and a tritium monitor TEM 2102A [Mab Solutions GmbH]. Whereas chemically bonded tritium remains in the solution (as HTO) and tritium activity was measured with liquid scintillation method. Solution containing tritium was distilled and 5 mL aliquot mixed with 15 mL of Ultima Gold scintillation cocktail and analysed for total tritium with a Tri-Carb 2910TR counter [PerkinElmer, Inc]. Amount of tritium atoms was calculated from its activity in Becquerel by means of the tritium decay constant [21]. Detailed description of the chemical processes occurring during the measurement and calculations are given in [19].

Thermal desorption of tritium was performed in a flow of He + 0.1% H₂ purge gas at 14–15 L/h. The quartz tube in the setup had two compartments – one for the sample in a porcelain boat and one for

Table 3
Comparison of tritium measurement techniques - dissolution and thermal desorption.

	Dissolution	TDS
Information obtained	<ul style="list-style-type: none"> • tritium total amount • depth profile • chemical state (T⁰, TH, TD, T₂ in gas phase, T⁺ - in liquid phase) 	<ul style="list-style-type: none"> • Tritium total amount • Desorption spectra
Tritium release method	Be dissolution in 1 M H ₂ SO ₄ simultaneous hydrogen measurement	Be heating in a furnace, ~5 °C/min up to 1030 °C and held 1 h at this temperature
Carrier gas	Argon	Helium + 0,1% H ₂
Tritium measurement	Proportional counter – gas phase Liquid scintillation – liquid phase	Proportional counter

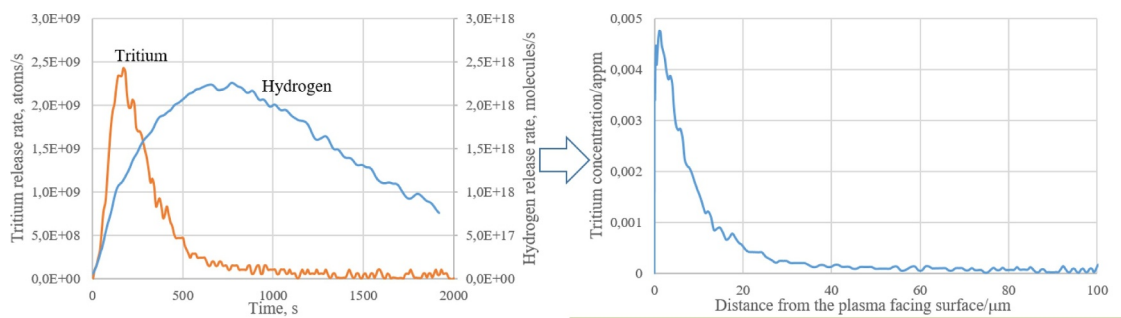


Fig. 3. Tritium depth profile measurement data (on the left) and depth profile (on the right) for sample from IWGL tile No 75 (ILW1).

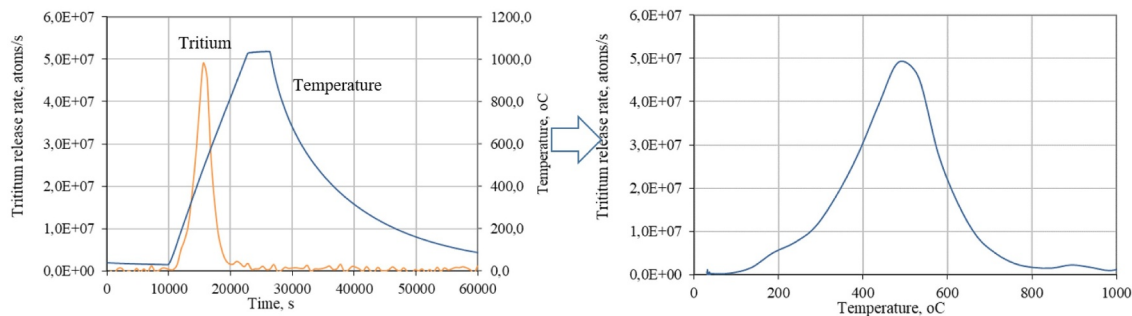


Fig. 4. Tritium thermal desorption spectra measurement data (on the left) and desorption spectra (on the right) for sample from IWGL tile No 75 (ILW1).

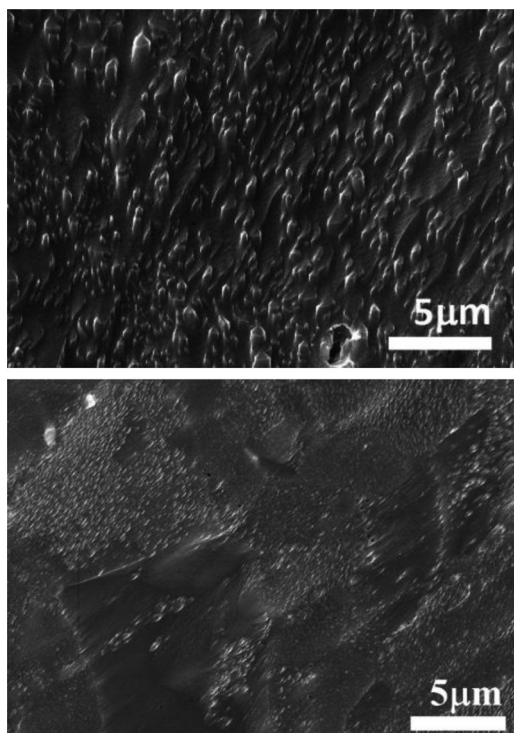


Fig. 5. Prolonged beryllium structures on the plasma facing surface of the central part of the IWGL tile, sample from the ILW1 on the left (sample No 41) and from ILW2 on the right (sample No 207).

a bed of granulated zinc. The quartz cap had a thermocouple channel – an inner quartz tube sealed towards the sample. The zinc bed at 665–675 converts tritiated water to molecular gaseous tritium (HT, DT, and traces of T₂). Samples were heated at a rate of 4.8 K/min to 1305 K and then kept at that temperature for 1 h. The temperatures of the sample, the zinc bed and the cold trap were continuously measured. The tritium activity in the purge gas was continuously monitored using a proportional counter with an operating volume of 300 cm³ and a tritium monitor TEM 2102A. As the subsequent second heating of the same sample in the same setup with the same temperature program to 1303 K caused no appreciable tritium release, the final value of the tritium sum release in the first heating was defined as a total tritium release. Comparison of the two techniques for tritium measurements in beryllium are given in Table 3 and Figs. 3 and 4.

3. Results

3.1. Structure of the plasma facing surfaces

Surface structure and chemical composition of the plasma facing surfaces were assessed by the means of scanning electron microscope equipped with the EDX detector. Surface structure differs not only depending on tile position in the vacuum vessel but also across single tiles. Structure of the samples from central part of the tile from inner wall guarding limiter IWGL indicates direct interaction with plasma as there can be observed prolonged beryllium structures that are similar to the surface morphology of beryllium exposed to the light ion in plasma device Pisces-B [22]. Whereas both side parts of the particular tile have scale like deposition layer that according to EDX data contains nickel, oxygen, carbon and traces of tungsten and iron. Similar surface structure was observed in both campaigns - ILW1 and ILW2 (Fig. 5).

Similar to the IWGL tile also central part of WPL tile have prolonged beryllium structures, whereas left hand side part of the tile has melted/resolidified Be layer or droplets rich in oxygen on the surface (Fig. 6), whereas samples from the right hand part have a nickel interlayer used

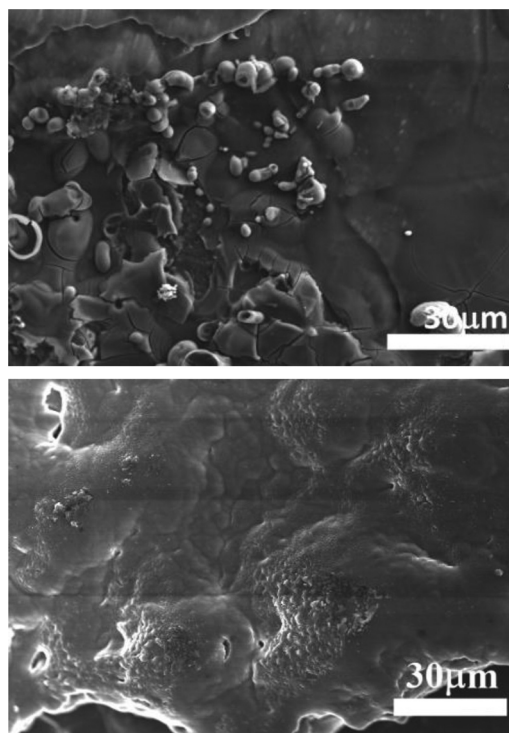


Fig. 6. Melted/resolidified beryllium layer rich in oxygen on the surface of the samples from the left side of the WPL tile sample from the ILW1 on the left (sample No 165) and from ILW2 on the right (sample No 365).

in erosion experiments that are visible due to the cracked and delaminated upper layer of beryllium. Delamination of the Ni layer was also observed (Fig. 7).

3.2. Tritium content

Tritium total content was assessed by dissolution and thermal desorption methods for ILW1 samples and by dissolution method for ILW 2 samples. Tritium thermal desorption spectra of the samples from ILW1 are already published in [19].

Tritium surface concentration ranges from $2 \cdot 10^{11}$ – $2 \cdot 10^{13}$ atoms per square centimetre of the surface area. Lowest tritium concentration was found in the sample from tile of the upper part of the vacuum vessel (DP - 2BC2) - $2.0 \cdot 10^{12}$ atoms/cm² and $2.0 \cdot 10^{11}$ atoms/cm² in ILW1 and ILW2, respectively. Highest tritium concentration is in samples from outer wall tile (WPL - 4D14) - up to $1.9 \cdot 10^{13}$ atoms/cm² in ILW1 campaign and $2.4 \cdot 10^{13}$ atoms/cm² ILW2 (average values $1.1 \cdot 10^{13}$ and $1.6 \cdot 10^{13}$ atoms/cm²). In inner wall tile (IWGL - 2XR10) tritium concentration is considerably lower with its higher concentration $3.8 \cdot 10^{12}$ atoms/cm² in ILW1 and $2.3 \cdot 10^{12}$ atoms/cm² ILW2 (average values $2.6 \cdot 10^{12}$ and $1.6 \cdot 10^{12}$ atoms/cm²). Tritium content in different parts of inner and outer wall tiles after ILW1 and ILW2 campaigns are compared in Figs. 8 and 9.

In the tile from the inner wall there is a decrease of tritium content after ILW2 if to compare with ILW1 in all measured parts of the tile, however its distribution tendency remains similar with its lowest concentration in the central part of the tile which according to the SEM and EDX results has been exposed to the material loss. In the tile from outer wall tritium content is slightly higher after the ILW2, however similar to the inner wall tile the tendency of the distribution across the tile remains the same, except for the sample 114/314. Tritium content is considerably lower in the part of tile where Ni interlayer was present (samples 106/306).

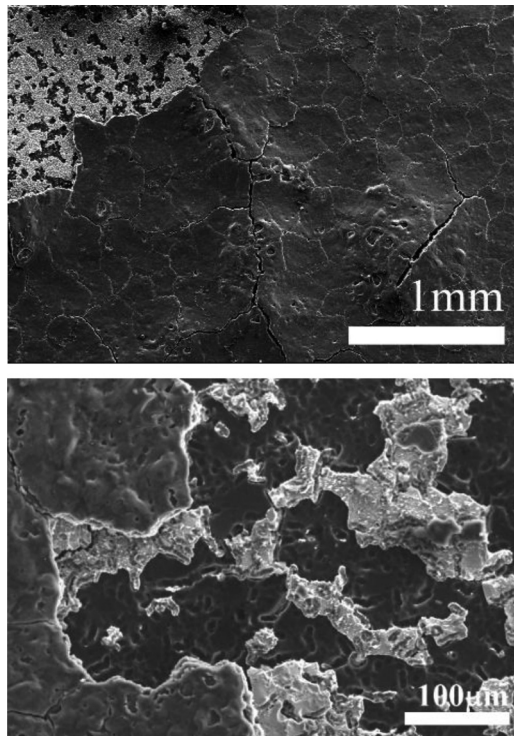


Fig. 7. Delaminated Be and Ni layers on the surface of sample from WPL tile side part (small magnification picture of the sample No 106 on the right and larger of the 306 on the left).

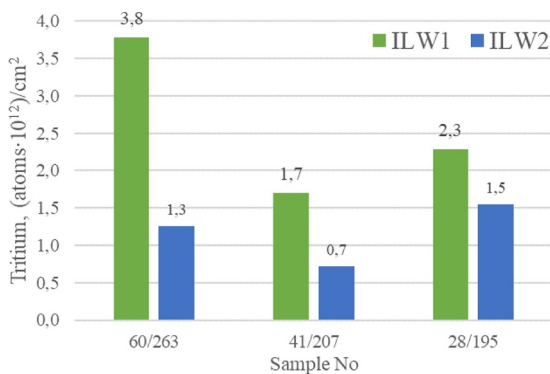


Fig. 8. Tritium content in different parts of the inner wall tile IWGL 2XR10.

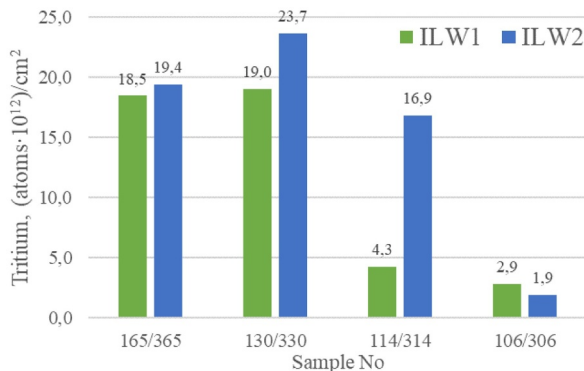


Fig. 9. Tritium content in different parts of the outer wall tile WPL 4D14.

4. Discussion

Tritium concentration in the beryllium tiles differs significantly regarding the tile position in the vacuum vessel. There is more tritium accumulated in the outer wall tiles than that in inner wall or upper part to the vessel. If to compare obtained results with deuterium content in particular tiles published in [23], it can be seen that there are large differences. According to [23] total deuterium content in the tiles retrieved in 2012 shutdown (ILW1) IWGL (2XR10), WPL (4D14) and DP (2BC2) tiles is $1.13 \cdot 10^{20}$, $1.14 \cdot 10^{20}$ and $2.1 \cdot 10^{22}$ atoms, respectively, whereas tritium average surface concentrations for the same tiles are $2.6 \cdot 10^{12}$, $11.2 \cdot 10^{12}$ and $2.0 \cdot 10^{12}$ atoms/cm². Deuterium distribution is more uniform regarding its concentration in outer and inner wall, whereas for tritium there is 5 times more tritium in outer wall than that in inner wall. These differences indicate different accumulation mechanisms of tritium and deuterium that could be linked to the different sources of the two isotopes. Deuterium has been introduced into the vacuum vessel during the campaigns, whereas tritium comes from the sources described in the Section 1. (in-vessel tritium inventory remaining from previous D – T campaigns, energetic tritium ion production as a result of D – D reaction and tritium production in neutron induced transmutation of beryllium). Tritium diffusion into the bulk of the material might have significant role. Tritium concentration differences are linked also to the plasma surface interactions - there is more tritium in the tile parts where melted material has been transferred and is rich with oxygen (for example, 60/263 in the IWGL 2XR10 tile). It has been observed that beryllium oxidation increases hydrogen isotope retention as it becomes chemically bonded in the bulk of the material [24].

Less tritium where deuterium concentration is the highest might be related to the isotope exchange process - tritium being “washed out” by deuterium. In the ILW2 there is even less tritium in the upper part - that could be linked to the hydrogen phase when considerable amounts of hydrogen has been puffed inside the vessel.

To predict tritium accumulation patterns in ITER and other future fusion devices tritium - deuterium plasma experiments are crucial as fuel accumulation highly depends of the way how it is introduced in the vacuum vessel.

Conclusions

- Tritium content is higher in the outer wall Be limiter tiles ($11.2 \cdot 10^{12}$ and $15.5 \cdot 10^{12}$ atoms/cm² after ILW1 and ILW2, respectively) than that in inner wall ($2.6 \cdot 10^{12}$ and $1.6 \cdot 10^{12}$ atoms/cm²) and upper region tiles ($2.0 \cdot 10^{12}$ - $2.0 \cdot 10^{11}$ atoms/cm²) in both campaigns.
- If to compare ILW1 and ILW2 tritium content in the beryllium wall materials is similar on average, however its distribution across the vacuum vessel is more uneven in ILW2.
- Tritium distribution in vacuum vessel is different from deuterium distribution. Lowest tritium concentration is observed where highest deuterium concentration has been reported.

Acknowledgements

This work has been carried out within the framework of the EUROfusion Consortium and has received funding from the EURATOM research and training programme 2014–2018 under grant agreement No. 633053. The views and opinions expressed herein do not necessarily reflect those of the European Commission

References

- [1] L. Horton, The JET ITER-like wall experiment: first results and lessons for ITER, *Fusion Eng. Des.* 88 (6) (2013) 434–439.
- [2] G. Federici, et al., Beryllium as a plasma facing material for near-term fusion devices, Reference Module in Materials Science and Materials Engineering, Elsevier,

- Oxford, 2016.
- [3] M.J. Rubel, et al., Beryllium plasma-facing components for the ITER-like wall project at JET, *J. Phys. Conf. Ser.* 100 (6) (2008) 062028.
- [4] H. Maier, et al., Tungsten and beryllium armour development for the JET ITER-like wall project, *Nucl. Fusion* 47 (3) (2007) 222.
- [5] S. Krat, et al., Erosion at the inner wall of JET during the discharge campaign 2013–2014, *Nucl. Mater. Energy* 11 (2017) 20–24.
- [6] G. De Temmerman, et al., Efficiency of thermal outgassing for tritium retention measurement and removal in ITER, *Nucl. Mater. Energy* 12 (2017) 267–272.
- [7] J.E.T. Team, Fusion energy production from a deuterium-tritium plasma in the JET tokamak, *Nucl. Fusion* 32 (2) (1992) 187.
- [8] M. Keilhacker, et al., High fusion performance from deuterium-tritium plasmas in JET, *Nucl. Fusion* 39 (2) (1999) 209.
- [9] J. Jacquinot, et al., Overview of ITER physics deuterium-tritium experiments in JET, *Nucl. Fusion* 39 (2) (1999) 235.
- [10] K.D. Zastrow, et al., Tritium transport experiments on the JET tokamak, *Plasma Phys. Control. Fusion* 46 (12B) (2004) B255.
- [11] D. Stork, et al., Overview of transport, fast particle and heating and current drive physics using tritium in JET plasmas, *Nucl. Fusion* 45 (10) (2005) S181.
- [12] M.G. Ganchenkova, V.A. Borodin, R.M. Nieminen, Hydrogen in beryllium: solubility, transport, and trapping, *Phys. Rev. B* 79 (13) (2009) 134101.
- [13] R. Kaur, S. Prakash, Isotope effect for hydrogen diffusion in metals, *J. Phys. F Met. Phys.* 12 (7) (1982) 1383.
- [14] R.A. Causey, Hydrogen isotope retention and recycling in fusion reactor plasma-facing components, *J. Nucl. Mater.* 300 (2–3) (2002) 91–117.
- [15] J.E. Evans, Reaction Products in High NVT Irradiated Beryllium, Phillips Petroleum Co. Atomic Energy Div., Idaho Falls, Idaho, 1956 Medium: ED; Size: Pages: 11.
- [16] A.V. Fedorov, et al., Analysis of tritium retention in beryllium pebbles in EXOTIC, PBA and HIDOBE-01 experiments, *J. Nucl. Mater.* 442 (1, Supplement 1) (2013) S472–S477.
- [17] A. Widdowson, et al., Experience of handling beryllium, tritium and activated components from JET ITER like wall, *Phys. Scr.* 2016 (T167) (2016) 014057.
- [18] K. Heinola, et al., Experience on divertor fuel retention after two ITER-Like Wall campaigns, *Phys. Scr.* 2017 (T170) (2017) 014063.
- [19] E. Pajuste, et al., Structure, tritium depth profile and desorption from 'plasma-facing' beryllium materials of ITER-Like-Wall at JET, *Nucl. Mater. Energy* 12 (2017) 642–647.
- [20] E. Pajuste, et al., Tritium distribution and chemical forms in the irradiated beryllium pebbles before and after thermoannealing, *Fusion Eng. Des.* 86 (9–11) (2011) 2125–2128.
- [21] L.L. Lucas, M.P. Unterwieser, Comprehensive Review and Critical Evaluation of the Half-Life of Tritium, *J. Res. Natl Inst. Stand. Technol.* 105 (4) (2000) 541–549.
- [22] R.P. Doerner, M.J. Baldwin, D. Nishijima, Plasma-induced morphology of beryllium targets exposed in PISCES-B, *J. Nucl. Mater.* 455 (1) (2014) 1–4.
- [23] K. Heinola, et al., Long-term fuel retention in JET ITER-like wall, *Phys. Scr.* 2016 (T167) (2016) 014075.
- [24] C. Makepeace, et al., The effect of Beryllium Oxide on retention in JET ITER-like wall tiles, 23rd International Conference on Plasma Surface Interactions, Princeton, USA., 2018, p. 392.